HHS Public Access

Author manuscript

Stem Cells. Author manuscript; available in PMC 2009 April 09.

Published in final edited form as:

Stem Cells. 2007 February ; 25(2): 411–418. doi:10.1634/stemcells.2006-0380.

Enhanced Yield of Neuroepithelial Precursors and Midbrain-Like Dopaminergic Neurons from Human Embryonic Stem Cells Using the Bone Morphogenic Protein Antagonist Noggin

Kai-Christian Sonntag, **Jan Pruszak**, **Takahito Yoshizaki**, **Joris van Arensbergen**, **Rosario Sanchez-Pernaute**, and **Ole Isacson**

Center for Neuroregeneration Research, Udall Parkinson's Disease Center of Excellence, McLean Hospital, Harvard Medical School, Belmont, Massachusetts, USA

Abstract

It is currently not known whether dopamine (DA) neurons derived from human embryonic stem cells (hESCs) can survive in vivo and alleviate symptoms in models of Parkinson disease (PD). Here, we report the use of Noggin (a bone morphogenic protein antagonist) to induce neuroectodermal cell development and increase the yield of DA neurons from hESCs. A combination of stromal-derived inducing activity and Noggin markedly enhanced the generation of neuroepithelial progenitors that could give rise to DA neurons. In addition, Noggin diminished the occurrence of a fibroblast-like Nestin-positive precursor population that differentiated into myocytes. After transplantation of differentiated hESCs to a rodent model of PD, some grafts contained human midbrain-like DA neurons. This protocol demonstrates hESC derivation and survival of human DA neurons appropriate for cell therapy in PD.

Keywords

Human embryonic stem cells; Dopamine; Differentiation; Noggin; Parkinson's disease 6-Hydroxydopamine-lesioned rats

INTRODUCTION

The production of in vivo functional dopamine (DA) neurons from human embryonic stem cells (hESCs) is at an early stage of technological development. Although DA neurons can be derived from hESCs in vitro [1–8], there is some evidence that these neurons do not survive in vivo after transplantation [5, 8]. In addition, hESC differentiated cell populations prepared for transplantation contain pluri- and/or multipotent precursors that can give rise to unwanted cell types and grow into teratomas [6, 8]. When antagonizing bone morphogenic protein (BMP) signaling during early embryogenesis, Noggin reduces epidermal and

Correspondence: Kai-Christian Sonntag, M.D., Ph.D., Harvard Medical School, Center for Neuroregeneration Research, MRC 126, McLean Hospital, 115 Mill Street, Belmont, Massachusetts 02478, USA. Telephone: 617-855-3138; Fax: 617-855-3284; e-mail: kai.sonntag@mclean.arvard.edu.

DISCLOSURES

The authors indicate no potential conflicts of interest.

mesodermal cell development, promoting the default pathway of neural induction [9]. These effects have provided the rationale for the use of Noggin in hESC differentiation protocols to enhance neuroectodermal cell development [10–12]. We now demonstrate that Noggin markedly increases the formation of neuroectodermal cells from hESCs in coculture with stromal feeder cells, which can enhance the production of specific DA neurons appropriate for future transplantation therapies for Parkinson disease (PD).

MATERIALS AND METHODS

hESC Culture and In Vitro Differentiation

The work with hESCs was approved by the Partners ESCRO (Embryonic Stem Cell Research Oversight) Committee under protocol number 2006-04-001A. hESC lines H7 (WA-07, XX, passages P29–P35) and H9 (WA-09, XX, approximately passage 35) were cultured according to the guidelines established by the National Academy of Sciences. Cells were propagated on mitomycin-C (10 μg/ml for 150 minutes; Sigma-Aldrich, St. Louis, http://www.sigmaaldrich.com)-inactivated human (D551; American Type Culture Collection, Manassas, VA, http://www.atcc.org) fibroblasts in serum replacement medium (SRM) (Dulbecco's modified Eagle's medium [DMEM], 15% knockout serum replacement; Invitrogen Corporation, Carlsbad, CA, http://www.invitrogen.com). Differentiation of hESCs was adapted from previously published protocols [4]. Briefly, neuroectodermal differentiation ("rosette formation") of hESCs was induced by coculture on transgenic MS5-Wnt1 stromal feeder cells (Dr. L. Studer, Sloan-Kettering Institute, New York). hESCs were triturated and plated in a density of approximately 0.5–1 colonies per six-well plate on a confluent layer of mitotically inactivated MS5-Wnt1 cells using SRM for 14 days, followed by N2 medium (DMEM/F-12; Invitrogen Corporation) (N2-A; Stem Cell Technologies, Vancouver, BC, Canada, http://www.stemcell.com). Neuroectodermal induction was achieved either without or with the addition of 300 ng/ml Noggin (R&D Systems, Inc., Minneapolis, http://www.rndsystems.com) for 7 (1 week) or 21 (3 weeks) days to the culture medium (Fig. 1A). Media were changed every 2 days, and cells were differentiated toward the DA phenotype in the presence of growth factor combinations as follows: 200 ng/ml sonic hedgehog (SHH), 100 ng/ml fibroblast growth factor 8 (FGF8) (both R&D Systems, Inc.), 20 ng/ml brain-derived neurotrophic factor (BDNF) (PeproTech EC Ltd., London, http://www.peprotechec.com), 20 ng/ml basic fibroblast growth factor (bFGF) (Invitrogen Corporation), 1 ng/ml transforming growth factor type β3 (TGF-β3) (Calbiochem, San Diego, http://www.emdbiosciences.com), 10 ng/ml glial cell line-derived neurotrophic factor (GDNF), 0.5 mM dibutyryl cAMP, and 0.2 mM ascorbic acid (AA) (all from Sigma-Aldrich). At day 21 of differentiation, rosettes were harvested mechanically from feeders and gently replated on 15 μg/ml polyornithine plus 1 μg/ml laminin-coated culture dishes in N2 medium supplemented with bFGF, BDNF, AA, SHH, and FGF8. After 9 days (day in vitro 30 [DIV30]) cells were passaged using 0.05% trypsin/EDTA (Invitrogen Corporation) and spun at 1,000 rpm for 5 minutes. Cells were resuspended in N2 medium and plated again at a density of approximately 50,000–100,000 cells per square centimeter on polyornithine/laminin-coated dishes in the absence of bFGF but in the presence of BDNF, AA, SHH, and FGF8. After an additional 7 days of culture (DIV37), cells were

differentiated until DIV42 or DIV49 in the absence of SHH and FGF8 but in the presence of BDNF, AA, cAMP, GDNF, and TGF-β3.

Immunocytochemistry and Immunohistochemistry

Cells were analyzed by immunofluorescence staining as previously described [13, 14] and examined using an LSM510 Meta confocal microscope equipped with ultraviolet, argon, and helium-neon lasers (Carl Zeiss, Thornwood, NY, http://www.zeiss.com). The following primary antibodies were used: sheep anti-tyrosine hydroxylase (TH) (1:300) from Pel-Freez, Rogers, AK, http://www.invitrogen.com; rabbit polyclonal anti-glial fibrillary acidic protein (GFAP) (1:500) from Dako North America, Carpinteria, CA, http://www.dakousa.com; goat polyclonal anti-GFAP (1:300), rabbit polyclonal anti-β-III-tubulin (TuJ1) (1:2,000), and rabbit polyclonal anti-Pax2 from Covance, Princeton, NJ, http://www.covance.com; neuronal nuclei (1:100), rabbit polyclonal anti-Sox1 (1:300), and rabbit polyclonal anti-nestin (1:300) from Chemicon International, Temecula, CA, http://www.chemicon.com; goat polyclonal anti-Otx2 (1:1,000) from Neuromics, Edina, MN, http://www.neuromics.com; rabbit anti-5HT (1:5,000) from DiaSorin S.p.A., Saluggia, Italy, http://www.diasorin.com; mouse immunoglobulin G2b (IgG2b) anti-myosin (MF20) (1:300), mouse IgM anti-forebrain surface embryonic marker 1 (FORSE-1) (1:80), and mouse polyclonal anti-engrailed-1 (En-1) (1:40) from Developmental Studies Hybridoma Bank, Iowa City, IA, http://www.uiowa.edu; and rabbit polyclonal anti-brain factor-1 (BF-1) (1:1,000) (Dr. L. Studer). To identify human cells in the rodent brain, we used the human-specific antibody against human nuclear antigen (1:50; Chemicon International). The appropriate fluorescent-labeled secondary antibodies (Alexa Fluor goat or donkey anti-rabbit, -mouse, or -sheep 488, 568, 594, 647; Invitrogen Corporation) (1:500) were applied for visualization, and nuclei were counterstained with Hoechst 33342 (5 μg/ml; Invitrogen Corporation). On selected sections, the primary antibody was omitted to verify specificity of staining.

Fluorescence-Activated Cell Sorting Analysis

Cells were harvested at the immature stage (by mechanical selection) and at DIV21 and DIV42 using 0.05% trypsin/EDTA. After gentle trituration, cells were filtered through cell-strainer caps to obtain a single-cell suspension. Surface antigens were labeled by incubating for 50 minutes with the following primary antibodies: mouse IgM anti-stage-specific embryonic antigen (SSEA)-1 (0.4 μg/ml) and mouse IgM anti-SSEA-4 (3 μg/ml) from Developmental Studies Hybridoma Bank; mouse IgM anti-Tra-1-60 (15 μg/ml) from Chemicon International; mouse IgG1 anti-neural cell adhesion molecule (NCAM) (Eric-1; 1:100) from Santa Cruz Biotechnology, Inc., Santa Cruz, CA, http://www.scbt.com, and with fluorescent-labeled secondary antibodies as above. All washing steps were performed in Hanks' balanced salt solution (Invitrogen Corporation) containing penicillin-streptomycin, 20 mM glucose, and 2% fetal bovine serum. The stained cells were analyzed on a FACSAria (BD Biosciences, San Jose, CA, http://www.bdbiosciences.com), and data analysis was performed using FlowJo software (TreeStar Inc., Ashland, OR, http://www.treestar.com).

Cell Counts

Quantitative immunocytochemical analysis was performed on randomly selected visual fields from at least two independent differentiation experiments. In each field, images of separate channels (Hoechst, 488, 568, 594) were acquired at ×40 magnification on an integrated epifluorescence microscope (Axioskop 2+; Carl Zeiss) using the StereoInvestigator image capture equipment and software (MBF Bioscience, Inc., Williston, VT, http://www.mbfbioscience.com) and exported to an imaging software (Adobe Photoshop; Adobe Systems Incorporated, San Jose, CA, http://www.adobe.com), where separate channel images as well as the corresponding overlaid images were counted. On average, 20–25 visual fields were acquired per 16-mm coverslip, and a total of 4,000–8,000 Hoechst$^+$ cells were counted per experiment in a blinded manner by two investigators. The total numbers of TH$^+$, GFAP$^+$, MF20$^+$, and "Nestin-flat" cells were then plotted as the percentage of total Hoechst$^+$ cells. Areas were measured on confocal images from coverslips to estimate nuclear/cytoplasm ratios in flat and slender Nestin$^+$ cells. Multinuclear cells were not included.

Reverse Transcription-Polymerase Chain Reaction and Quantitative Real-Time Polymerase Chain Reaction

Reverse transcription-polymerase chain reaction (RT-PCR) was performed as described [13] using the following published primer pairs: β-actin [2]; TH, Nurr1, and Pitx-3 [1]; Sox1 and En1 [6]; Oct4 [15]; Pax2 [16]; Pax6 and Nestin [17]; Msx1 [18]; and Lmx1a [19].

For quantitative real-time (Q)-PCR, cDNA samples (approximately 25–50 ng/μl mRNA equivalent) were analyzed using the SYBR Green Jumpstart Taq ReadyMix (Sigma-Aldrich) and an Opticon MJ thermocycler (MJ Research, now part of Bio-Rad, Hercules, CA, http://www.bio-rad.com) in total volumes of 25 μl with 40 nmol primers for each reaction. Linearity and detection limit of the assay were performed in 10-fold serial dilutions (linear curves $r \geq .9$) to determine optimal template amounts. Quantification was performed at a threshold detection line ("threshold cycles," Ct value). The Ct of each gene product (TH, βIII-tubulin, and heavy chain myosin [HCM]) was normalized against that of the housekeeping gene β-actin, which was run simultaneously for each marker. Data were expressed as mean ± SEM. The ΔCt for each candidate was calculated as ΔCt of [Ct (candidate) – Ct (GAPDH)] according to the methods of Livak et al. [20] and plotted as relative levels of gene expression. Data were analyzed by a two-tailed Student's *t* test, and statistical significance was set at $p < .05$. For the Q-PCR, the following additional primers were used: βIII-tubulin 5′-TGGATTCGGTCCTGGATGTG-3′ (forward) and 5′-ACCTTGCTGATGAGCAACGT-3′ (reverse), β-actin 5′-CCTTGCACATGCCGGAG-3′ (reverse), and HCM [21].

Transplantation into the Striatum of 6-Hydroxydopamine-Treated Rats

Animal studies were approved by the Institutional Animal Care and Use Committee at McLean Hospital and Harvard Medical School. Unilateral 6-hydroxydopamine (6-OHDA)-lesioned adult female Sprague-Dawley rats (200–250 g) were purchased from Taconic (Taconic Farms Inc., Germantown, NY, http://www.taconic.com). As described elsewhere [22, 23], 2 μl (2 μg/μl) of 6-OHDA were stereotaxically injected into the right median

forebrain bundle. After purchase, rats were screened by apomorphine rotation at Taconic and tested for amphetamine-induced rotation (2.5 mg/kg) in our laboratory at least 6 weeks after lesion. Rats that demonstrated more than 700 turns after drug injection were considered to have more than 97% striatal DA lesion and were selected for cell transplantation. Rotational behavior in response to amphetamine (4 mg/kg i.p.) was evaluated before transplantation and at 9 and 12 weeks after transplantation as described [22, 23].

Differentiated H7 and H9 hESCs were gently trypsinized into a cell suspension, counted, and resuspended at approximately 25,000 viable cells per microliter in the final differentiation medium. Four microliters were slowly injected into the lesioned striatum of the rats (anteroposterior = 0 lat = −2.8 from bregma, and from −5.5 to −4.5 mm ventral from dura, with the tooth bar set at −3.3). Injections were performed as previously described [14, 24]. Rats were immunosuppressed with cyclosporine-A (15 mg/kg per day, Sandimmune; Sandoz, Princeton, NJ, http://www.us.sandoz.com) starting 1 day prior to surgery. Three months after transplantation, animals were terminally anesthetized, and the brains were removed, fixed, and analyzed using multiple-immunofluorescence labeling as described [14]. Cell counts of TH^+ neurons were performed on every 12th section by using an Axioplan microscope (Carl Zeiss) under a ×40 lens. Only stained cells with visible dendrites were counted as neurons, and counts from serial sections were corrected and extrapolated for whole graft volumes using the Abercrombie method [25].

RESULTS

hESCs were first differentiated in vitro on the mouse stromal cell line MS5-Wnt1, and then neural precursors were grown in feeder-free conditions with factors supporting DA cell development and survival [4] (Fig. 1A). In our hands, this protocol did not produce sufficient amounts of neural progenitors from the National Institutes of Health (NIH)-approved cell lines H7 and H9 for further in vitro differentiation and in vivo transplantation experiments. By DIV21, hESCs developed into populations of heterogeneous cell types growing in “crater-like” structures (Fig. 1B). In contrast, addition of Noggin to the MS5 cocultures (Fig. 1A) produced more homogeneous colonies with a remarkable increase in neuroectodermal rosette-like structures (Fig. 1B), which could be expanded in the absence of the MS5 stromal cells (Fig. 2A, left panel). Previous reports have suggested that such rosettes represent neural plate-like [4] and/or neural tube-like precursor cells [7, 26]. Accordingly, cultured rosettes (DIV35) expressed the neural tube and radial-glia marker 3CB2 [27] in their center part and the neuronal marker Tuj1 at their edges, indicating their immature and neuronal differentiation properties (Fig. 2A, right panel). The rosettes also expressed the neural precursor markers Nestin and Sox1 and the midbrain marker Otx2 with or without Pax2 [28, 29] (Fig. 2B), whereas only a few cells coexpressed Pax2 and En-1 (not shown). Rosettes expressing the forebrain marker BF-1 (foxg1) [30] coexpressed the forebrain surface-embryonic marker 1 (FORSE-1) [31] (Fig. 2B). At the early stage of differentiation, we noted the appearance of some TH-positive neurons. These neurons were scattered and preferentially located at the interface between the MS5 stromal cells and the rosette-containing ESC colonies (supplemental online Fig. S1).

The neuroepithelial cells from manually collected rosettes were cultured in conditions favoring neurogenesis and DA neuronal differentiation [4] (Fig. 1A and Fig. 3A). At DIV37, $Tuj1^+/TH^+$ DA neurons [4] had developed and RT-PCR experiments revealed that the DA neurons in both Noggin culture conditions exhibited similar gene expression profiles for the DA- and midbrain-associated markers TH, Nurr1, Pitx3, En-1, Pax2, Lmx1a, and Msx1 [29, 32, 33] (Fig. 3B). To estimate the efficiency of DA neuronal cell development, we performed cell counts that revealed an approximately twofold increase in the numbers of TH^+ neurons in the 3-week compared with the 1-week Noggin treatment at DIV37 and 49 (Fig. 3C). In addition, Q-PCR analysis showed that the gene expression levels for Tuj1 were increased in the 3-week Noggin condition at DIV37 and 49 (Fig. 3D). Q-PCR analyses also showed an approximately threefold increase in TH expression in the 3-week Noggin conditions, but these differences could not be observed at DIV 49 (Fig. 3D). However, when the TH gene expression levels were normalized against the corresponding Tuj1 levels, an overall increase was observed in the 3-week Noggin conditions (Fig. 3D). We also observed the presence of heavy myofilament 20 (MF20)- and GFAP-positive cells (Fig. 4C and supplemental online Fig. 2A). Quantification of the $MF20^+$ cells at DIV37 and 49 demonstrated a marked decrease with 3-week (<1%) compared with 1-week Noggin treatment (6%–7%), which was consistent with gene expression levels for HCM as determined by Q-PCR (Fig. 3E). In contrast, the numbers of $GFAP^+$cells increased slightly in the 3-week Noggin-treated cultures (Fig. 3E). Using fluorescence-activated cell sorting (FACS), we analyzed the fractions of cells that expressed the immature cell markers Tra-1-60, SSEA-4, and SSEA-1 and the neural marker NCAM at various stages of differentiation (Fig. 3F). From the ESC stage to rosette formation (DIV21), there was an approximately 97% reduction of $Tra\text{-}1\text{-}60^+$ and an approximately fourfold increase of $SSEA\text{-}1^+$ cells (Fig. 3F). At DIV42, approximately 75% of the cells in the cultures were NCAM-positive and there was a small fraction of cells (<1%) that expressed the immature markers SSEA-4 and SSEA-1 in the 3-week Noggin treatment conditions (Fig. 3F). Using RT-PCR, low levels of the marker Oct4 and a persistent expression of the neural precursor marker Sox1 were also detected at this time (Fig. 3C).

We observed the presence of two morphologically distinct $Nestin^+$ cell populations. One population, which was present in both Noggin conditions and represented the majority, consisted of small cells with scarce cytoplasm (nuclear/cytoplasma ratio 0.638 ± 0.016) and one or two slender, long processes (“Nestin-slender”) (Fig. 4). The other phenotype had a “fibroblast-like,” flat morphology with larger cytoplasm (nuclear/cytoplasm ratio 0.281 ± 0.015), thick and short processes, and occasional multinuclearity (Nestin-flat). The Nestin-flat phenotype was predominantly present in the 1-week Noggin condition and did not appear before DIV37 (Fig. 4). Quantification of the Nestin-flat cells confirmed a larger number in the 1-week than in the 3-week Noggin-treated cultures (Fig. 4F). Characterization of the $Nestin^+$ cell populations at DIV49 demonstrated that a few Nestin-slender cells costained with the neuronal marker Tuj1, but not with GFAP or MF20, whereas many Nestin-flat cells were also positive for GFAP or MF20 (Fig. 4C–4E). Vimentin, another intermediate filament, was colocalized with GFAP in some, but not all, of these flat cells (data not shown). In addition, the Nestin-slender cells coexpressed the radial-glia marker 3CB2 and some of them were also positive for GFAP (supplemental online Fig. 2B),

indicating that these cells resemble radial-glia-like immature neural precursors. In summary, Noggin treatment reduced the presence of non-neural Nestin$^+$ precursors during differentiation.

To determine whether DA neurons from the in vitro differentiation would function in vivo, we harvested cells at DIV42 from the high-yield 3-week Noggin cultures from either the hESC line H9 or H7 (see Material and Methods for details) and transplanted them into the striatum of hemi-parkinsonian rats (6-OHDA lesioned). In the group of rats that received differentiated cells from H9 hESCs (n = 8), rotational behavior in response to amphetamine was unchanged (average response to amphetamine increased by 24% ± 9% at 12 weeks; n = 5). Three animals had very large grafts (larger than striatum) and were sacrificed before the completion of the study. Postmortem analyses revealed only very few DA neurons in the grafts (1–3 TH$^+$ cells in two grafts) (Fig. 5A–5D), serotonin (5HT$^+$) neurons (data not shown), pluripotent SSEA-4$^+$ immature precursors (Fig. 5E), and non-neural components, including MF20$^+$ cells (Fig. 5F). In contrast, in the group receiving H7 hESC-derived cells (n = 12), three animals showed variable degrees of behavioral improvement at 9 and 12 weeks from 10%–94% reduction in amphetamine-induced rotation (Fig. 5G). In two of these animals (Fig. 5G), an initial contralateral rotation was observed in the first minutes after amphetamine administration, which is typically seen only for functional DA grafts [34]. Altogether, nine animals had surviving grafts that contained multiple cell types, including TH$^+$ neurons (average 160 ± 74; n = 7) (Fig. 5A–5D). Two animals that died before the end of the study had large teratomas, which also contained TH$^+$ neurons (not quantified). The TH$^+$ cells (Fig. 5C, 5D) appeared individually or in clusters and had a cell soma size ranging from 20 to 50 μm, which is consistent with an average size (37 μm) of midbrain DA neurons in grafts of PD patients after receiving human fetal cell transplantation [35]. In addition, some of these TH$^+$ cells coexpressed G-protein-gated inwardly rectifying K$^+$ channel 2 (Girk2), a typical marker for DA neurons in the human substantia nigra pars compacta (A9 region) (data not shown) [35] and had complex neurites with relatively little outgrowth into the host striatum.

DISCUSSION

This study demonstrates that a combination of stromal cell coculture and the BMP antagonist Noggin markedly enhanced the development of two hESC lines (H7 and H9) into neuroectodermal precursors. Differentiation of these precursors in culture conditions favoring DA neurogenesis demonstrated an increase in the amount of midbrain-like DA neurons. We also found that these culture conditions reduced the formation of fibroblast-like Nestin$^+$ mesodermal progenitors. Moreover, in a rodent model of PD, DA neurons were present in grafts of animals that were transplanted with cells differentiated from the H7 ESCs. However, despite of the reduction in mesodermal precursors, surprisingly, the transplantation experiments also revealed the presence of teratoma, which included MF20$^+$ myocytes (discussed below).

Successful use of ESC-derived DA cells to alleviate symptoms in animals models of PD has been demonstrated for mouse (reviewed in [36]) and primate ESCs [37]; however, data from hESCs is currently limited. There are only a few published studies that report transplantation

of differentiated hESCs in animal models [1, 3, 5, 6], and in two publications teratoma formation was reported [6, 8]. In the current study, we also observed teratoma-like grafts after transplantation of differentiated cells at DIV42, and this was independent of the hESC source (H7 or H9). Thus, the in vitro differentiation conditions in our studies did not completely avert the persistence of proliferative toti- and/or pluripotent precursors. The characteristics of these precursors are not clear. Two scenarios are envisioned. First, the presence of a totipotent "stem-like" cell that does not respond to these inductive signals and can form teratoma in vivo. This is supported by the RT-PCR and the FACS analyses demonstrating low levels of Oct4 expression, a low percentage (<1%) of SSEA-4$^+$ and Tra-1-60$^+$ cells at DIV42, and the presence of SSEA-4$^+$ cells in some of the grafts. Second, the presence of several heterogeneous populations of pluri- and/or multipotent progenitors. For example, there were two morphologically distinct Nestin$^+$ cell types, which segregated into neural-like (Nestin-slender) cells that appeared to be radial-glia-like precursors giving rise to neurons and astroglia and mesodermal (Nestin-flat) progenitors [38]. Whereas the mesodermal Nestin-flat cells developed at later stages of differentiation, at the early stages (rosettes) Nestin was coexpressed with Sox1, a marker for neuroepithelial cells at the closure of the neural tube [39]. In the 3-week Noggin condition, Sox1 was continuously and highly expressed during in vitro differentiation. Moreover, in this condition, the development of MF20$^+$ cells was decreased, but their occurrence was not prevented in vivo. An interpretation of these results suggests that, under these conditions, Noggin produced a common precursor and reduced its development into the mesodermal lineage. Interestingly, SMA$^+$ (smooth muscle actin-positive) smooth muscle cells [1] and teratoma formation [8] have been described in brain grafts from transplanted hESCs after differentiation in PA6 cocultures. This indicates that non-neural precursors can also develop in other stromal cell-derived inducing activity (SDIA)-based in vitro differentiation paradigms.

The characteristics of the rosettes in the Noggin conditions were similar to those described recently by other investigators [4, 7, 26] and resembled radial-glia-like neural tube cells. This indicates that the addition of Noggin to the cultures does not seem to alter the common phenotypes of neuroepithelial-like precursors, which express markers typical for dorso-ventral and anterior-posterior patterning. In addition, the expression of the forebrain markers FORSE-1 and BF-1 (foxg1) implied the presence of neural precursors that potentially could give rise to cortical neurons [30].

When differentiated cells were transplanted into the striatum of parkinsonian rats, we observed functional DA neurons that had the typical morphology and phenotype of midbrain DA neurons in grafts from PD patients who received fetal cell transplantation [35]. This indicates that hESCs differentiated with our protocol have the potential to produce the appropriate and therapeutically relevant DA cell population that survive in vivo as stable phenotype for at least 12 weeks. Interestingly, these neurons developed only from H7 hESCs, but not from H9 hESCs. The reason for this discrepancy is not known and there is no obvious explanation for this result, except of heterogeneity of the human stem cell lines. Previously, after transplantation of undifferentiated ESCs from the NIH-approved cell lines H1 (WA-01) and HES4 (ES04), we observed that TH$^+$ DA neurons developed as part of teratomas within 5 weeks after engraftment (R. Sanchez-Pernaute and O. Isacson, unpublished results). Therefore, we believe that all these hESC lines have an intrinsic

capacity to differentiate into DA neurons, although differences may exist in their ability to produce surviving and functional cells. In other hESC in vitro differentiation and transplantation paradigms, none [5] or few surviving TH^+ neurons have been reported [1, 3, 6, 8], and evidence for functional DA neurons was described only by Ben-Hur et al. [3]. In their protocol, the DA cells developed without the use of DA-specific culture conditions in hESC-derived neurospheres that were later transplanted. Interestingly, a correlation between behavioral recovery and presence of TH^+ neurons in the striatum showed that, in two animals, approximately 600 cells were necessary to obtain approximately 80% reduction in amphetamine-induced rotation [3]. This is consistent with our results showing that marked recovery (94%) occurred only in the presence of 560 TH^+ neurons.

SUMMARY

We demonstrate a protocol combining the inductive properties of MS5-Wnt1-based SDIA with Noggin, which markedly increased the development of neuroepithelial precursors giving rise to human midbrain-like DA progenitors and/or neurons that can function in vivo, although it does not entirely eliminate stem cells and/or precursors, which can develop into other tissue. These results indicate both the potential and the need for further improvements of hESC differentiation protocols toward the isolation and/or enrichment of (homogeneous) DA cell populations for cell replacement therapy in PD.

Supplementary Material

Refer to Web version on PubMed Central for supplementary material.

ACKNOWLEDGMENTS

We thank Dorothy Kester, Shreeya Karki, Gabriella Brunlid, and Benjamin Holmes for excellent technical help and Dr. Lorenz Studer for providing the MS5-Wnt1 stromal cells and the BF-1 antibody. This study was supported by National Institute of Neurological Disorders and Stroke Udall Ctr. P50 NS-39793, Michael Stern Foundation for Parkinson's Disease Research, Orchard Foundation, Consolidated Anti-Aging Foundation, and the Harvard Stem Cell Institute.

REFERENCES

1. Zeng X, Cai J, Chen J, et al. Dopaminergic differentiation of human embryonic stem cells. STEM CELLS. 2004; 22:925–940. [PubMed: 15536184]
2. Buytaert-Hoefen KA, Alvarez E, Freed CR. Generation of tyrosine hydroxylase positive neurons from human embryonic stem cells after coculture with cellular substrates and exposure to GDNF. STEM CELLS. 2004; 22:669–674. [PubMed: 15342931]
3. Ben-Hur T, Idelson M, Khaner H, et al. Transplantation of human embryonic stem cell-derived neural progenitors improves behavioral deficit in Parkinsonian rats. STEM CELLS. 2004; 22:1246–1255. [PubMed: 15579643]
4. Perrier AL, Tabar V, Barberi T, et al. Derivation of midbrain dopamine neurons from human embryonic stem cells. Proc Natl Acad Sci U S A. 2004; 101:12543–12548. [PubMed: 15310843]
5. Park CH, Minn YK, Lee JY, et al. In vitro and in vivo analyses of human embryonic stem cell-derived dopamine neurons. J Neurochem. 2005; 92:1265–1276. [PubMed: 15715675]
6. Schulz TC, Noggle SA, Palmarini GM, et al. Differentiation of human embryonic stem cells to dopaminergic neurons in serum-free suspension culture. STEM CELLS. 2004; 22:1218–1238. [PubMed: 15579641]

7. Yan Y, Yang D, Zarnowska ED, et al. Directed differentiation of dopaminergic neuronal subtypes from human embryonic stem cells. STEM CELLS. 2005; 23:781–790. [PubMed: 15917474]
8. Brederlau A, Correia AS, Anisimov SV, et al. Transplantation of human embryonic stem cell-derived cells to a rat model of Parkinson's disease: Effect of in vitro differentiation on graft survival and teratoma formation. STEM CELLS. 2006; 24:1433–1440. [PubMed: 16556709]
9. Munoz-Sanjuan I, Brivanlou AH. Neural induction, the default model and embryonic stem cells. Nat Rev Neurosci. 2002; 3:271–280. [PubMed: 11967557]
10. Pera MF, Andrade J, Houssami S, et al. Regulation of human embryonic stem cell differentiation by BMP-2 and its antagonist noggin. J Cell Sci. 2004; 117:1269–1280. [PubMed: 14996946]
11. Gerrard L, Rodgers L, Cui W. Differentiation of human embryonic stem cells to neural lineages in adherent culture by blocking bone morphogenetic protein signaling. STEM CELLS. 2005; 23:1234–1241. [PubMed: 16002783]
12. Itsykson P, Ilouz N, Turetsky T, et al. Derivation of neural precursors from human embryonic stem cells in the presence of noggin. Mol Cell Neurosci. 2005; 30:24–36. [PubMed: 16081300]
13. Sonntag KC, Simantov R, Bjorklund L, et al. Context-dependent neuronal differentiation and germ layer induction of Smad4−/− and Cripto−/− embryonic stem cells. Mol Cell Neurosci. 2005; 28:417–429. [PubMed: 15737733]
14. Sanchez-Pernaute R, Studer L, Ferrari D, et al. Long-term survival of dopamine neurons derived from parthenogenetic primate embryonic stem cells (cyno-1) after transplantation. STEM CELLS. 2005; 23:914–922. [PubMed: 15941857]
15. Tai MH, Chang CC, Kiupel M, et al. Oct4 expression in adult human stem cells: Evidence in support of the stem cell theory of carcinogenesis. Carcinogenesis. 2005; 26:495–502. [PubMed: 15513931]
16. Silberstein GB, Dressler GR, Van Horn K. Expression of the PAX2 oncogene in human breast cancer and its role in progesterone-dependent mammary growth. Oncogene. 2002; 21:1009–1016. [PubMed: 11850818]
17. Jang YK, Park JJ, Lee MC, et al. Retinoic acid-mediated induction of neurons and glial cells from human umbilical cord-derived hematopoietic stem cells. J Neurosci Res. 2004; 75:573–584. [PubMed: 14743441]
18. Ginis I, Luo Y, Miura T, et al. Differences between human and mouse embryonic stem cells. Dev Biol. 2004; 269:360–380. [PubMed: 15110706]
19. Thameem F, Wolford JK, Wang J, et al. Cloning, expression and genomic structure of human LMX1A, and variant screening in Pima Indians. Gene. 2002; 290:217–225. [PubMed: 12062816]
20. Livak KJ, Schmittgen TD. Analysis of relative gene expression data using real-time quantitative PCR and the 2(-Delta Delta C(T)) Method. Methods. 2001; 25:402–408. [PubMed: 11846609]
21. Wicks J, Haitchi HM, Holgate ST, et al. Enhanced upregulation of smooth muscle related transcripts by TGF beta2 in asthmatic (myo) fibroblasts. Thorax. 2006; 61:313–319. [PubMed: 16449267]
22. Bjorklund LM, Sanchez-Pernaute R, Chung S, et al. Embryonic stem cells develop into functional dopaminergic neurons after transplantation in a Parkinson rat model. Proc Natl Acad Sci U S A. 2002; 99:2344–2349. [PubMed: 11782534]
23. Costantini LC, Cole D, Chaturvedi P, et al. Immunophilin ligands can prevent progressive dopaminergic degeneration in animal models of Parkinson's disease. Eur J Neurosci. 2001; 13:1085–1092. [PubMed: 11285005]
24. Kim JH, Auerbach JM, Rodriguez-Gomez JA, et al. Dopamine neurons derived from embryonic stem cells function in an animal model of Parkinson's disease. Nature. 2002; 418:50–56. [PubMed: 12077607]
25. Abercrombie M. Estimation of nuclear populations from microtome sections. Anat Rec. 1946; 94:239–247. [PubMed: 21015608]
26. Li XJ, Du ZW, Zarnowska ED, et al. Specification of motoneurons from human embryonic stem cells. Nat Biotechnol. 2005; 23:215–221. [PubMed: 15685164]
27. Prada FA, Dorado ME, Quesada A, et al. Early expression of a novel radial glia antigen in the chick embryo. Glia. 1995; 15:389–400. [PubMed: 8926034]

28. Hynes M, Rosenthal A. Specification of dopaminergic and serotonergic neurons in the vertebrate CNS. Curr Opin Neurobiol. 1999; 9:26–36. [PubMed: 10072377]
29. Vitalis T, Cases O, Parnavelas JG. Development of the dopaminergic neurons in the rodent brainstem. Exp Neurol. 2005; 191(suppl 1):S104–S112. [PubMed: 15629757]
30. Martynoga B, Morrison H, Price DJ, et al. Foxg1 is required for specification of ventral telencephalon and region-specific regulation of dorsal telencephalic precursor proliferation and apoptosis. Dev Biol. 2005; 283:113–127. [PubMed: 15893304]
31. Tole S, Kaprielian Z, Ou SK, et al. FORSE-1: A positionally regulated epitope in the developing rat central nervous system. J Neurosci. 1995; 15:957–969. [PubMed: 7532706]
32. Andersson E, Tryggvason U, Deng Q, et al. Identification of intrinsic determinants of midbrain dopamine neurons. Cell. 2006; 124:393–405. [PubMed: 16439212]
33. Goridis C, Rohrer H. Specification of catecholaminergic and serotonergic neurons. Nat Rev Neurosci. 2002; 3:531–541. [PubMed: 12094209]
34. Costantini LC, Isacson O. Neuroimmunophilin ligand enhances neurite outgrowth and effect of fetal dopamine transplants. Neuroscience. 2000; 100:515–520. [PubMed: 11098114]
35. Mendez I, Sanchez-Pernaute R, Cooper O, et al. Cell type analysis of functional fetal dopamine cell suspension transplants in the striatum and substantia nigra of patients with Parkinson's disease. Brain. 2005; 128:1498–1510. [PubMed: 15872020]
36. Sonntag KC, Simantov R, Isacson O. Stem cells may reshape the prospect of Parkinson's disease therapy. Brain Res Mol Brain Res. 2005; 134:34–51. [PubMed: 15790528]
37. Takagi Y, Takahashi J, Saiki H, et al. Dopaminergic neurons generated from monkey embryonic stem cells function in a Parkinson primate model. J Clin Invest. 2005; 115:102–109. [PubMed: 15630449]
38. Wiese C, Rolletschek A, Kania G, et al. Nestin expression-a property of multi-lineage progenitor cells? Cell Mol Life Sci. 2004; 61:2510–2522. [PubMed: 15526158]
39. Pevny LH, Sockanathan S, Placzek M, et al. A role for SOX1 in neural determination. Development. 1998; 125:1967–1978. [PubMed: 9550729]

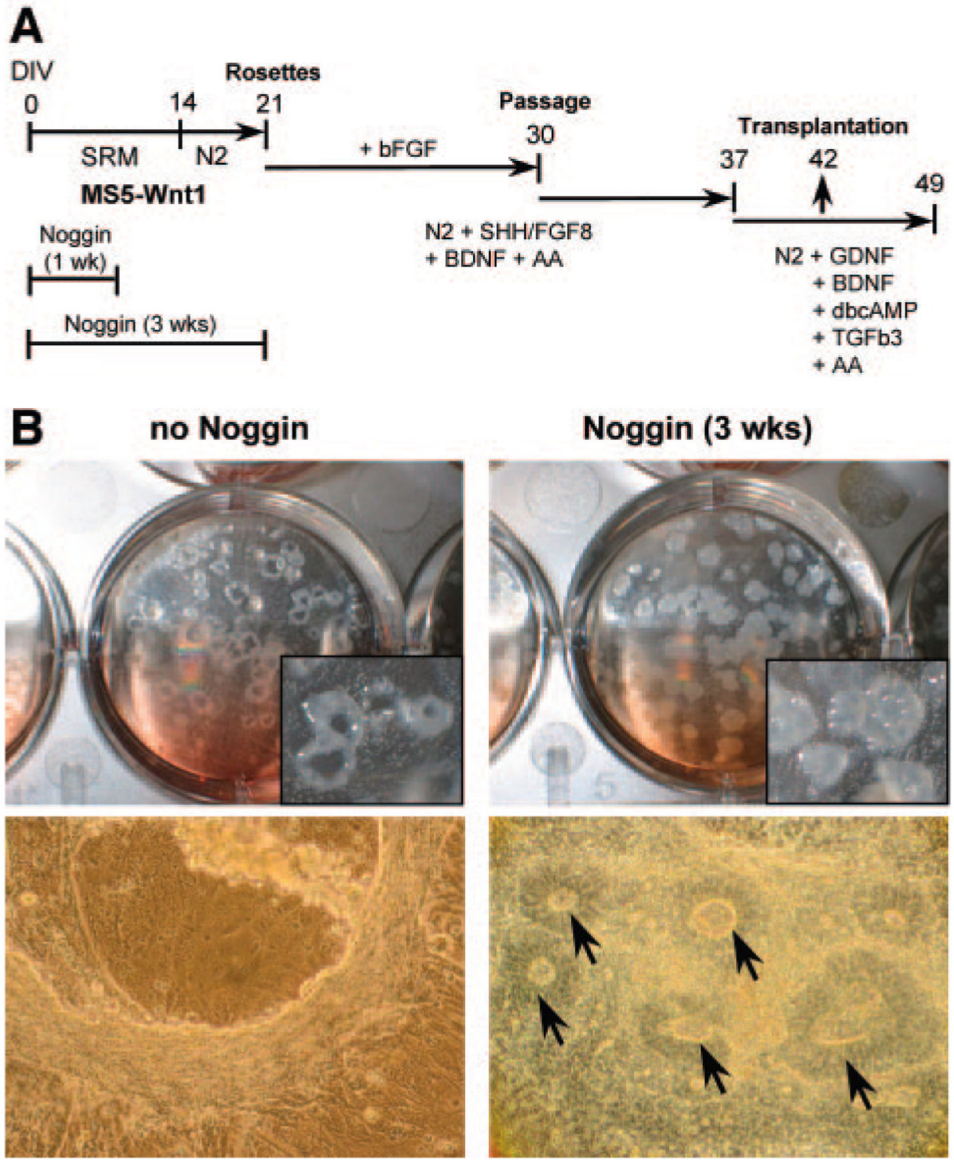

Figure 1.

Culture conditions and development of neuroectodermal cells. **(A):** Schematic representation of the protocol used to differentiate human embryonic stem cells (hESCs). hESCs were differentiated in a multistep protocol supporting dopamine neuronal cell development [4] and modified by adding 300 ng/ml Noggin during the stromal feeder cell-based neuroectodermal induction (DIV0–21) for either 1 week (DIV0–7) or 3 weeks (DIV 0–21). On DIV21, rosettes were selected and manually transferred to polyornithine/laminin-coated culture dishes, expanded, and further differentiated using the sequential addition of media supplements as indicated (see Material and Methods for further details). At DIV42, cells were harvested for transplantation into the striatum of 6-hydroxydopamine-treated rats. **(B):** The effects of Noggin on neuroectodermal cell development. Left panels: In the absence of Noggin, hESC colonies developed into typical crater-like structures with a single layer of homogeneous cells in the center and a rim with heterogeneous cellular

morphologies. In these conditions, the colonies had very little to no rosettes. An overview of colonies at low magnification and a representation of four colonies at higher magnification are shown in the inset (×5). Right panels: Addition of Noggin for 3-weeks led to increased formation of rosette-forming ESC colonies. An overview of colonies from Noggin-treated cultures at low magnification, which macroscopically appear homogeneous with a high cell density, is shown. Bright-field image (×5) of the border of a single colony at DIV21 showing an accumulation of rosettes (arrows). Abbreviations: AA, ascorbic acid; BDNF, brain-derived neurotrophic factor; bFGF, basic fibroblast growth factor; DIV, day in vitro; FGF8, fibroblast growth factor 8; SHH, sonic hedgehog; SRM, serum replacement medium; TGF-β3, transforming growth factor type β3.

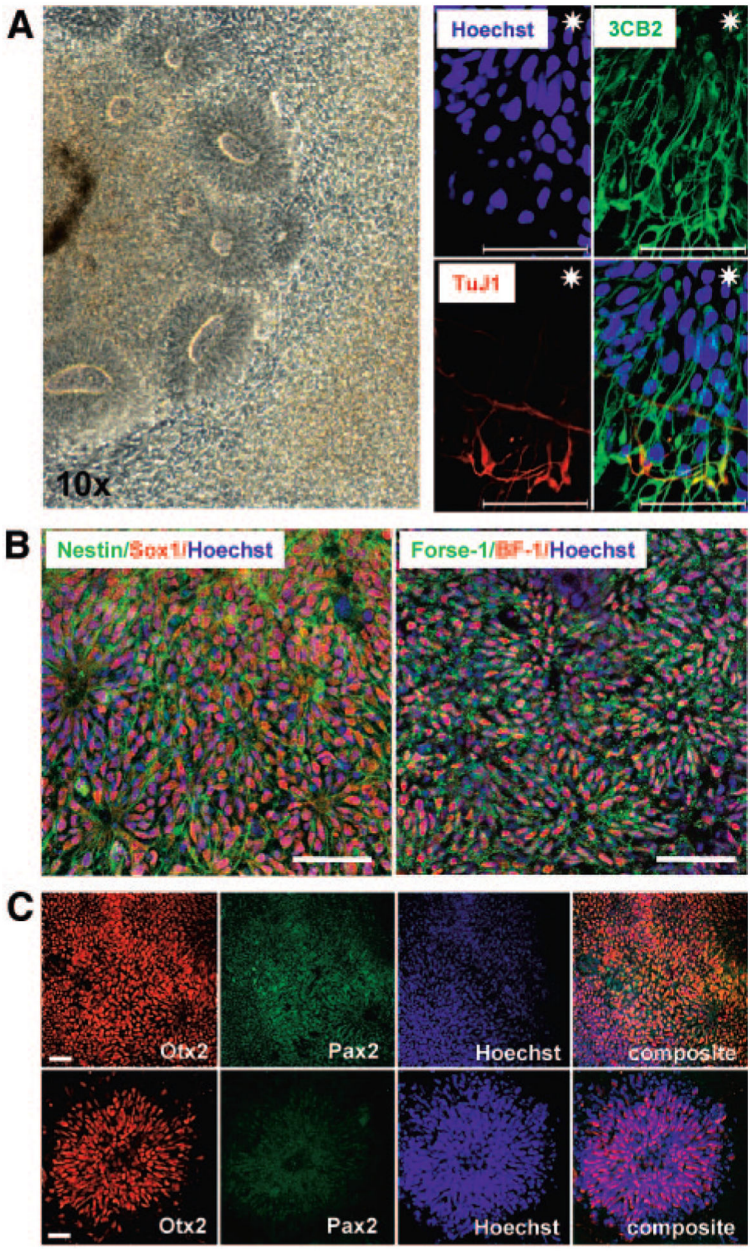

Figure 2.

Characterization of the neuroectodermal precursors. **(A):** Left panel: Bright-field image (×10) of cultured rosettes at day in vitro 30 (DIV30). Well-defined rosettes were surrounded by proliferating precursors. Right panel: Immunocytochemistry (ICC) images of rosettes using the nuclear marker Hoechst (blue), the radial-glia marker 3CB2 (green), and the neuronal marker Tuj1 (red). Shown is a part of a rosette with the center marked by a white star. Rosettes contained radial-glia-like cells in the center part and neurons at their edges. Scale bars = 50 μm. **(B):** ICC for the immature neural markers Sox1 (red) and Nestin (green). Rosettes were also stained with the forebrain-midbrain markers Otx2 (red), Pax2 (green) **(C),** and the forebrain markers FORSE-1 (green) and BF-1 (red) at DIV21. **(C):** In all culture conditions (Noggin for 1 week or 3 weeks), colonies were either $Otx2^{+}/Pax2^{+}$ or

$Otx^+/Pax2^-$. Scale bars = 75 μm (left set of images), 40 μm (right set of images).
Abbreviations: BF-1, brain factor-1; FORSE-1, forebrain surface embryonic marker 1.

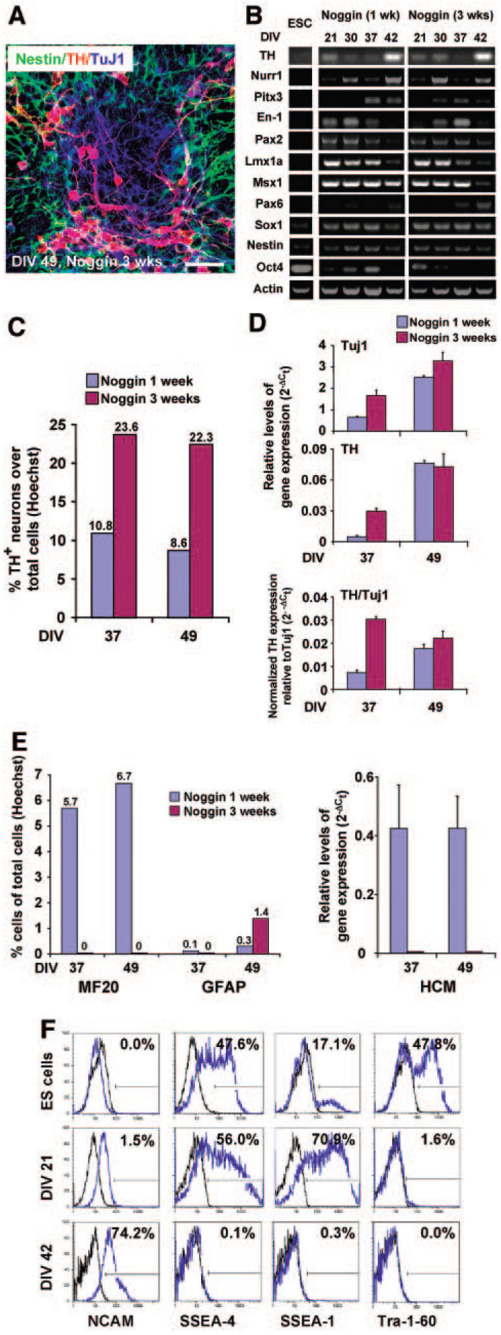

Figure 3.

The effect of Noggin on the development of neural and non-neural cellular phenotypes. **(A):** Dopamine (DA) neuronal cell development. Immunocytochemistry for Nestin (green), the neuronal marker Tuj1 (blue), the DA marker TH (red), and Hoechst at DIV49 in the 3-week Noggin conditions. Scale bars = 50 μm. **(B):** Gene expression profile during human embryonic stem cell (hESC) development. Reverse transcription-polymerase chain reaction (PCR) results from immature ESCs and cell samples at DIVs 21, 30, 37, and 42 for the 1-week or 3-week Noggin conditions. Samples were analyzed for markers related to the

midbrain DA neuronal phenotype (TH, Nurr1, Pitx3, En-1, Pax2, Lmx1a, and Msx-1), the anterior segment marker Pax6, the neural precursor markers Sox1 and Nestin, and the immature ESC marker Oct4. Shown is one representative out of three independent experiments. **(C):** Quantification of the TH^+ neurons at DIV37 and 49 in the Noggin 1-week (blue bars) and 3-week (red bars) conditions. Shown is one out of two experiments representing randomized cell counts of 4,000–8,000 $Hoechst^+$ cells for each experiment. The numbers of TH^+ cells are plotted as percentage of total cell counts as determined by Hoechst staining. **(D):** Quantitative real-time (Q)-PCR for Tuj1 and TH gene expression at DIV37 and 49. Relative gene expression levels were calculated using the $2^{-\Delta Ct}$ method according to Livak et al. [20] (upper and middle panels). In addition, the TH was normalized to the corresponding Tuj1 expression (lower panel). **(E):** Quantification of the $MF20^+$ and $GFAP^+$ cell populations at DIV37 and 49 in the Noggin 1-week (blue bars) and 3-week (red bars) conditions as described in **(B)** (left panel). Right panel: Q-PCR for human heavy chain myosin (HCM) plotted as relative levels of gene expression ($2^{-\Delta Ct}$) according to Livak et al. [20] **(F):** Detection of immature stem cells during hESC development in the 3-week Noggin condition. Fluorescence-activated cell sorting using specific antibodies for the stem cell markers SSEA-1, SSEA-4, and Tra-1-60, and the adhesion molecule NCAM at the immature ESC stage, DIV21 and 42. The numbers of immature ESCs substantially decreased during in vitro differentiation, whereas the fraction of $NCAM^+$ cells increased. Abbreviations: Ct, threshold cycle; DIV, day in vitro; ESC, embryonic stem cell; GFAP, glial fibrillary acidic protein; MF20, myosin; NCAM, neural cell adhesion molecule; TH, tyrosine hydroxylase; Tuj1, β-III-tubulin.

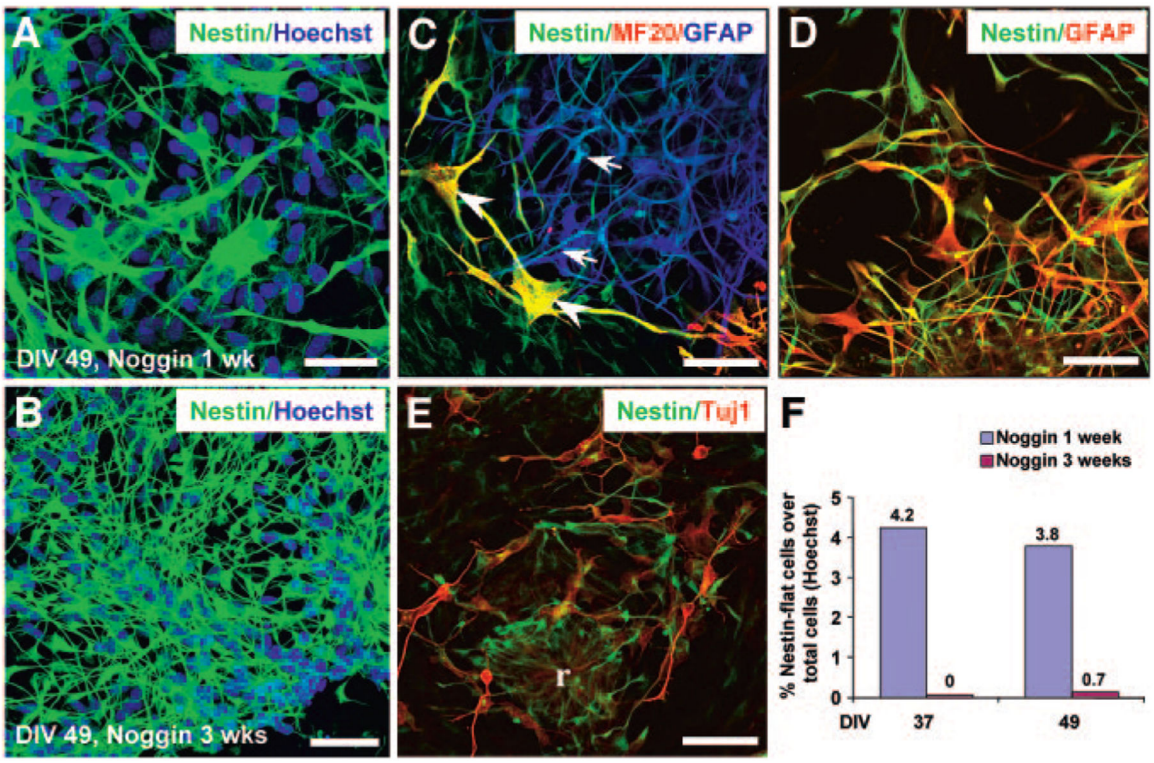

Figure 4.

The effects of Noggin on immature Nestin$^+$ progenitor cell development. Characterization of Nestin$^+$ cellular phenotypes at DIV49 in the 1-week **(A)** and 3-week **(B)** Noggin cultures. Scale bars = 50 μm. "Nestin-slender" cells were dominant and present in both culture conditions, whereas the "Nestin-flat" cells did not appear before DIV37 and occurred predominantly in the 1-week Noggin treatment condition. **(C–E):** Phenotype determination of the two Nestin$^+$ cell populations shows that Nestin-flat cells coexpress MF20 (arrow-heads) **(C)** and that some Nestin-slender cells coexpress Tuj1 **(E)**. GFAP is expressed in Nestin-flat cell populations **(D)** and arrows in **(C)**. Scale bars = 50 μm. **(F):** Quantification of the Nestin-flat cell populations at DIV37 and 49 for the 1-week and 3-week Noggin cultures. Cell counts were performed as described in the legend for Figure 3C and 3E. Abbreviations: DIV, day in vitro; GFAP, glial fibrillary acidic protein; MF20, myosin; Tuj1, β-III-tubulin.

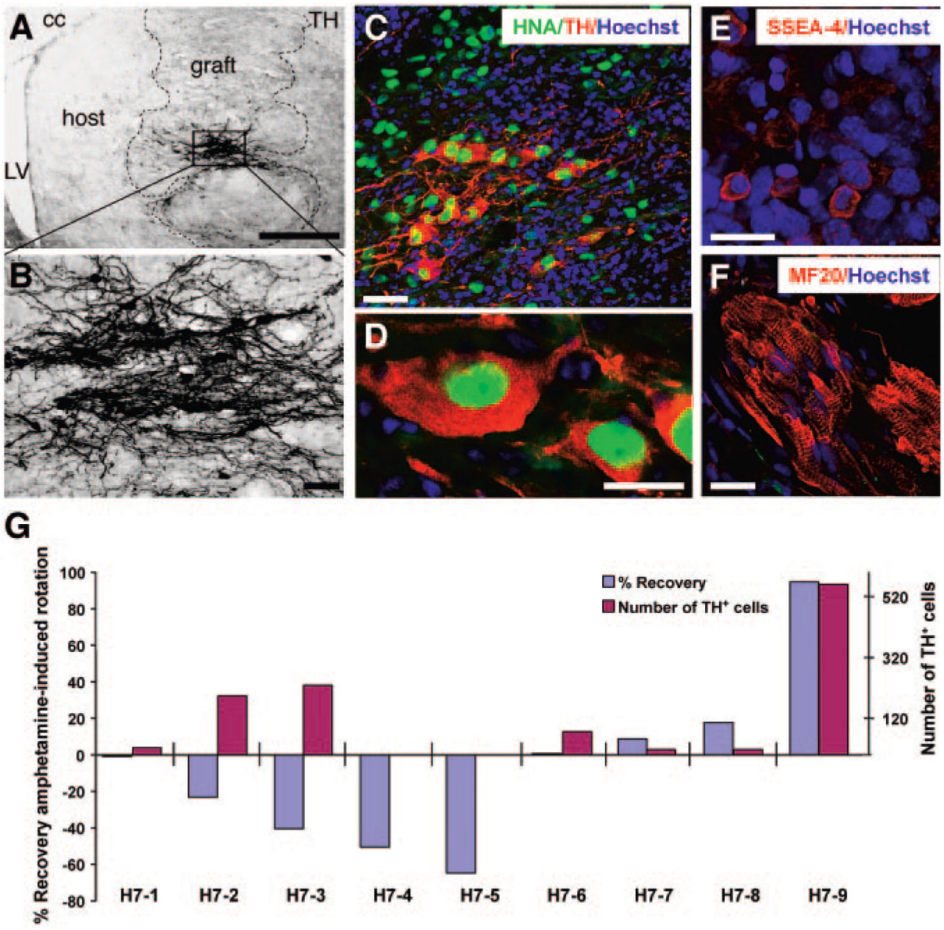

Figure 5.

Typical cellular phenotypes in grafts after transplantation of differentiated human embryonic stem cells (hESCs) (here, H7). **(A–F):** Immunocytochemistry revealed numerous surviving TH^+ neurons, sometimes in clusters, within the grafts in the 6-hydroxydopamine-lesioned rat striatum. These neurons had a mature morphology with big, polygonal cell soma (25–35 μm) and complex neuritic arborization. Scale bars = 1,000 μm **(A)**, 50 μm **(B)**. The TH^+ neurons were derived from hESCs as demonstrated by coexpression of human nuclear antigen (HNA) (green) and TH (red). Hoechst nuclear counterstain is shown in blue. Scale bars = 50 μm **(C)**, 25 μm **(D)**. The grafts also contained cells that stained with SSEA-4-specific antibodies (red), indicating the presence of pluripotent immature precursors **(E)**. Scale bar = 20 μm. **(F):** Example of non-neural multinucleated muscle cells within the graft (MF20 in red and Hoechst nuclear counterstain in blue). Scale bar = 40 μm. **(G):** Graphical representation of behavioral improvement in amphetamine-induced rotation (blue bars) paired with numbers of TH^+ neurons within grafts (red bars) of H7 hESC ($n = 9$) transplanted animals 12 weeks after implantation. Each set of bars represents data from one animal (H7-1 to H7-9). Abbreviations: cc, corpus callosum; LV, left ventricle; MF20, myosin; TH, tyrosine hydroxylase.